Radio Science, Volume 30, Number 5, Pages 1325–1339, September–October 1995

Numerical simulation of scatterer positions in a very dense medium with an application to the two-dimensional Born approximation

P. R. Siqueira, K. Sarabandi and F. T. Ulaby

Radiation Laboratory, University of Michigan, Ann Arbor

Abstract. Electromagnetic volume scattering theories for random media using a coherent field approach require some understanding of the statistical behavior of the locations of individual scatterers within the random medium. This knowledge manifests itself as the correlation function or pair distribution function, which is used to characterize the medium. This article presents a method for simulating the arrangements of particles of arbitrary shape within a very dense random medium, thus allowing for these functions to be calculated numerically. To demonstrate the significance of the Monte Carlo simulation, the problem of scattering from a two-dimensional dense random medium is considered. Using a first-order solution based on the Born approximation, it is shown that the approximate theoretically derived correlation function may lead to significant errors in the prediction of the backscatter response.

1. Introduction

Study of electromagnetic wave interaction with a collection of random particles (volume scattering) is of importance because of its application to a variety of radar remote sensing problems. Volume scattering theories are developed to determine basic electromagnetic properties of the medium such as the effective propagation constant, the attenuation constant, and the incoherent scattered power. Modeling efforts for volume scattering can be categorized into two groups: incoherent approaches and coherent approaches. In incoherent volume scattering theories, such as radiative transfer [*Chandrasekhar*, 1960], the effect of the phases of the fields scattered between neighboring particles is ignored. These methods are usually applied to sparse media where single scattering properties of constituent particles are used to formulate the volume scattering problem. Intensity approaches implicitly make the sparse medium assumption that individual scatterers are randomly positioned with respect to one another. As the scatterer density increases, multiple scattering between particles becomes, significant and the scattering solution based on the incoherent approach can become prohibitively complex [*Tsang and Ishimaru*, 1987]. Coherent approaches, on the other hand, such as the Born approximation and the quasi-crystalline approximation (QCA) [*Tsang et al.*, 1985], account for the interaction between particles through the inclusion of a permittivity fluctuation correlation function or a scatterer center pair distribution function, both of which provide statistical descriptions of the location of scatterers with respect to each other. The need for the correlation or pair distribution functions adds another complexity to volume scattering theories, namely that associated with how to determine these functions for the medium under consideration. These functions play an important role in determining the scattering behavior of the random medium and thus must be characterized accurately. The importance of this characterization has been somewhat overlooked in the literature. Simple Gaussian and exponential functions are usually used as an approximation for the correlation function since they are amenable for algebraic manipulation, but there is little evidence in support of the hypothesis that these are accurate representations of natural media. It is the purpose of this paper (1) to present a numerical

Paper number 95RS01760.
0048-6604/95/95RS-01760$08.00

technique to determine the correlation and pair distribution functions accurately and efficiently based on physical modeling of particle arrangements in a random medium; (2) to demonstrate the application of the correlation function to the two-dimensional Born approximation and make a comparison with theoretically derived results; (3) to use the derived correlation function to demonstrate limitations in the use of the exponential correlation function; and (4) to highlight the use of packing algorithms as a method of scattering analysis that can be used to analyze or enhance existing scattering theories.

The methods of determining the correlation function or the pair distribution function can be categorized into experimental theoretical, and numerical approaches. Experimental determination involves capturing an undisturbed sample of the volume under study and analyzing it for the desired information. This approach is quite difficult, very time consuming, and its accuracy depends on the particle size and measurement method. A classical example of such a process is given by *Vallese and Kong*[1981] where a layer of snow was infused with liquid plastic. The final result was the two-dimensional correlation function of the permittivity fluctuations due to the two dissimilar dielectrics of air and ice. The observed correlation function for one sample was then fit to a theoretical model (exponential) from which further calculations could be carried out. Further assumptions, such as azimuthal symmetry and validity of the theoretical model, were required to estimate the three-dimensional correlation function.

Theoretical methods of determining the correlation and pair distribution functions, while benefiting from a greater generality than experimental methods, must use simplifying assumptions to make the theories tractable and easy to handle. For the correlation function, it is common to use an exponential function [*Debye et al.*, 1957], which is derived by assuming that individual particles are positioned randomly with respect to one another. Such an assumption is valid in the limit when particle sizes are distributed over a wide range and/or when the particle density is low. This function will be the used as a basis of comparison further in the paper.

The pair distribution function of *Percus and Yevick*[1958] is another such theoretically derived function commonly used in conjunction with QCA and dense media radiative transfer [*Tsang and Ishimaru*, 1987]. This particular distribution is tailored for a medium consisting of discrete-sized spherical particles and in which there are no interparticle forces except exclusion, as in a classical fluid; external forces, such as gravity, are not taken into account. For macroscopic media such as snow, soils, and sand, the Percus-Yevick distribution may not be applicable because particle positions are dominated by forces such as friction, gravity, and inertia. It is not difficult to come up with examples where the Percus-Yevick pair distribution function would give considerably different results than would be expected for macroscopic particles under the influence of these conditions. For instance, if we were to create a dense assembly of uniform spheres in their lowest energy state, a crystal, and then randomly remove 10-20% of them, the pair distribution function would not change because the basic structure of the crystal still remains (see Appendix). In a classical fluid however, particles are allowed to rearrange themselves to reach the lowest energy state, which is dependent on their relation to one another. Thus the pair distribution function in a classical fluid would change as the Percus-Yevick distribution predicts, but there is no reason to expect that the pair distribution functions of macroscopic particles under a different set of forces would be similar. Thus it is important to explore other avenues of determining these functions to either verify the validity of employing these theoretical techniques to specific applications or generate the functions themselves.

Numerical methods refer to algorithms for determining the correlation function and pair distribution functions through the use of a computer to simulate the scatterer positions in a given space. Some of these methods are used to validate already existing theoretical distributions [*Ding et al.*, 1992; *Broyles et al.*, 1962], while others are used to determine the desired correlation or pair distribution functions directly [*Buchalter and Bradley*, 1992, 1994]. Packing algorithms are basically split into two groups, those that physically model the pouring deposition of particles and those that generate possible particle arrangements. Of the physical models of pouring, a general trend is to model the interaction of hard grains as they "pour" downward into a given volume. Models such as this are used to investigate local particle ordering and the effects of shaking packed sets of particles. The algorithm of *Buchalter and Bradley* is the most elaborate of these methods, it models collisions and rotations of uniform two-dimensional [1992] or three-dimensional [1994] monosized ellip-

soids as they pour into a two- or three-dimensional volume. Nevertheless, modeling of the physical pouring of particles is complex and time consuming; as this set of models more closely attempts to match the physical processes involved in the pouring process, the computation time will increase proportionally. For this reason, the numerical pouring model of physical deposition may not be appropriate for Monte Carlo simulations and may not be amenable to the real world situation of varying particle shape and size.

For the scattering problem, we may be more interested in computational efficiency in determining possible arrangements of particles rather than physically modeling their deposition if the resulting arrangement appears reasonable. In the arrangement set of algorithms, some methods, such as in the sequential addition method [*Ding et al.*, 1992], simply find open spaces for particles to fit within a confined area or incorporate an external force such as gravity, from which local potential energy can be minimized and particle stability can be maximized [*Visscher and Bolsterli*, 1972]. While the existing algorithms of this type can be considered to be much more computationally efficient than the physical deposition models, up until now they have been lacking in flexibility to model arrangements of particles of different shapes, particularly when it comes to the three-dimensional problem.

The method described here should be considered a method of generating particle arrangements rather than a numerical pouring model. It takes into account the three important factors of determining particle arrangements: nonpenetration of neighboring particles, gravity, and particle shape. This presented method is capable of determining particle distributions in both two and three dimensions and is computationally efficient enough to provide a large sample size for Monte Carlo simulations. The new method is not restricted to spherical/elliptically shaped particles and, as will be described, may be used in conjunction with coherent volume scattering theories to explore the scattering from dense random media.

This paper is arranged as follows: first the packing algorithm is described in section 2, and examples for both the two- and three-dimensional problems are given. Methods describing accurate calculation of the correlation function and pair distribution function from the computer-generated particle positions are given in section 3. In order to demonstrate the importance of the packing algorithm to the problem of volume scattering from a very dense medium, scattering solutions based on the Born approximation using the correlation function computed from the packing algorithm and an exponential function having the same correlation length are compared as a function of incidence angle and frequency. Because the angular backscatter response is proportional to the two-dimensional Fourier transform of the correlation function, it is possible to introduce the concept of a "visible region" where we can gain insight of how the choice of observation frequency samples the Fourier space of the correlation function. This is done in the second half of section 3, where the angular dependence of the backscatter response is demonstrated for a particular example at two different frequencies, one below and one above the resonance of the mean particle size. In the Appendix, we offer a brief discussion of the dependence of the pair distribution function on the particle arrangement method.

2. Packing Algorithm

We begin by introducing a user-defined distribution of particle states, $\mathbf{P}_p$, where the state of a particle is a vector representing the particle size, shape, orientation, and dielectric constant. For the purposes of demonstration, elliptically shaped particles will be used, however, this packing algorithm is not restricted to the simplified elliptical shapes. In two dimensions the state of such a particle is represented by

$$\mathbf{P}_p = (a_p, b_p, \theta_p, \epsilon_p) \tag{1}$$

where a_p, b_p are the lengths of the two principle axes, θ_p describes the orientation, and ϵ_p is the dielectric constant of the particle. To simulate the particle positions in two dimensions, a rectangular region with j being the discrete horizontal coordinate and z being the vertical coordinate is considered (Figure 1). Coordinates of the intersection of the principal axes of the particle p denote the position of the particle, which, together with the particle state, completely specifies the particle in the medium. The vector state of a particle is chosen by a random number generator with a prescribed distribution for the different states a_p, b_p, θ_p, and ϵ_p. In this paper, it is assumed that the principal axes of the particle have a normal distribution ($N(\overline{a}, \sigma_a)$) and the orientation angle of particles has a uniform distribution ($U(-\pi, \pi)$). The exact distributions of the particle states may be chosen according to physical measurements or an empirical

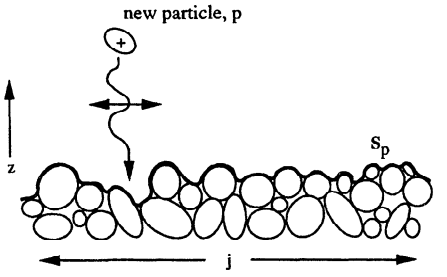

Figure 1. Illustration of the two-dimensional packing algorithm. Particles are fit to the surface S_p to find the minimum height, z. Once a particle has been fit to the surface, it becomes part of the surface for the next iteration of the process.

model. The particle is then laid down individually via the packing algorithm into the region to be filled. By making the limits of the region large compared to the sizes of the individual particles and by using the periodic boundary conditions, a semi-infinite layer of particles can be simulated. Periodic boundary conditions refer to making the spillover of a particle on one boundary appear on the opposite boundary of the region.

The packing algorithm starts by setting down an initial layer on the bottom of the rectangular region so that the lower surface is covered by a single layer of particles. This set of particles creates a bumpy solid surface, S_p. Particles are then sequentially added to the region in the following manner:

1. A particle state $\mathbf{P}_p$ is selected from the distribution, thus setting the particle shape and orientation.
2. The surface of the particle is discretized and then categorized into a set of lower and upper surface points, as shown in Figure 2. The points of the lower surface will be used in matching the surface of the particle to the current surface, S_p.
3. A fitting method is used to find the lowest height, z_p, as a function of the horizontal coordinates, that the particle will fit to the surface. This is equivalent to minimizing the potential energy of the particle.
4. The particle's position, $\bar{r}_p$, and state, $\mathbf{P}_p$, are stored in a file, and the surface is updated to S_{p+1} using the upper surface points determined in step two.
5. The first step is returned to until the desired layer thickness is reached.

The algorithm in its current state assumes that, averaged over a large sample, orientation is uniformly distributed between 0 and 2π. An additional complexity may be added to the algorithm to minimize z_p as a function of particle orientation also (i.e. θ is no longer one of the preset states given in (1)). While this may provide a more realistic variation to the algorithm, it is unlikely that the additional computational costs would outweigh the benefits. Biases in the orientation distribution that the user wishes to impose can be more efficiently introduced via the probability distribution chosen for the orientation states.

The fitting method described in step three is one of the key components that makes this algorithm computationally efficient. While any fitting method will be sufficient in this treatment, the one used here borrows a concept from the image processing technique of gray scale morphology [*Serra*, 1982; *Giardina and Dougherty*, 1988; *Appleton et al.*, 1993]. In this packing algorithm, a gray scale dilation is used to find the minimum height that a given shape fits to the surface. To describe this procedure, consider a particle such as the one shown in Figure 2. The surface of a particle is represented by an upper (M^{upper}) and a lower surface (M^{lower}). The lower part of the surface determines how the particle will fit the the current surface, S_p, and the upper part determines how the particle will contribute to the new surface, S_{p+1}, once the particle has been deposited. Given a parametric equation for the surface of a particle, $z_p(i)$, these surfaces can be described by

$$M_p^{\text{upper}}(i) = \{\max_z z_p(i) : -m \leq i \leq m\} \qquad (2)$$

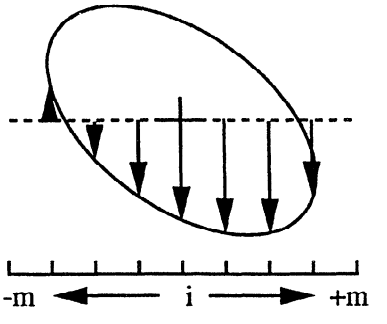

Figure 2. Illustration of the lower surface of a particle, M_p^{lower}. The particle is discretized into a horizontal grid and the maximum and minimum heights of the particle at points on the grid define the upper and lower surfaces.

$$M_p^{\text{lower}}(i) = \{\min_z z_p(i) : -m \leq i \leq m\} \quad (3)$$

where for a normally oriented ellipse, $z_p(i) = \pm b_p\sqrt{(1 - \frac{i^2}{a_p^2})}$, with a_p and b_p given in (1) and m being the horizontal limit of the extent of the ellipse ($m \geq \max(a_p, b_p)\ \forall p$). Note that the form of $z_p(i)$ is used here only for demonstration purposes and does not constrain the process once (2) and (3) have been determined.

The height of where a particle will rest for a given horizontal position, j, along the surface S_p is given by the morphological dilation (Figure 3)

$$\text{height}(j) = \{\max_i (S_p(j+i) - M_p^{\text{lower}}(i)) : -m \leq i \leq +m\}. \quad (4)$$

The minimum height attainable used by step three in the procedure is

$$z_p = \min_j (\text{height}(j)). \quad (5)$$

Successful algorithms have been implemented for both two- and three-dimensional elliptical particle distributions, and examples are shown in Figures 4 and 5 (to make the three-dimensional problem more efficient, a local minimization over an area of several particle diameters was performed rather than global minimization, indicated by (5)). The two-dimensional example clearly shows the algorithm's ability to generate very dense arrangements of particles in a short amount of computer time, two characteristics that make the algorithm amenable to Monte Carlo dense media volume scattering analysis. Furthermore, an analogous dense medium three- dimensional example is given for nonspherical particles with a Gaussian size distribution.

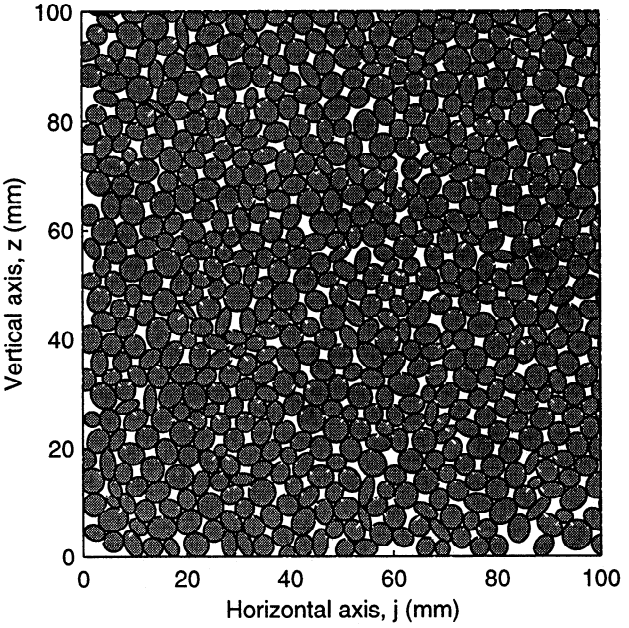

Figure 4. Demonstration of the two-dimensional packing algorithm. Particle radius is 2mm ± 0.4mm. In this case the volume fraction is 0.8. This particular simulation took 23 seconds on a Sun 10 workstation.

Results from the packing algorithm can be used to determine physical characteristics such as volume fraction, correlation length and function, and pair distribution function, of a volume under study. Future work in this area may be to include impurities such as water and determine the coating of individual grains through the implementation of simple physical processes such as surface tension and entropy max-

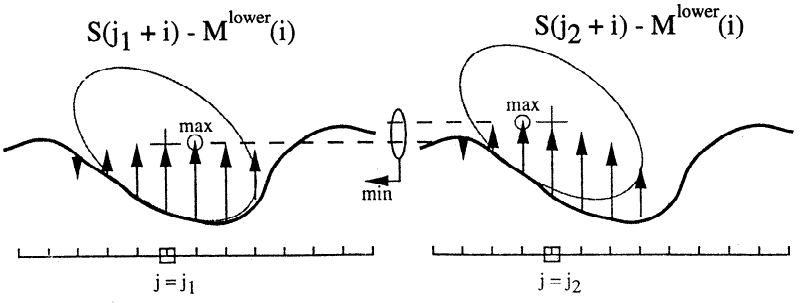

Figure 3. Illustration of (4) for two different points (j_1, j_2) on the surface $S(j)$. The dilation of the surface is shown for each point on the surface where the maximum is highlighted by a circle. This is the height of where the center of the ellipse would lie for a given horizontal location, j. The minimum of these heights defines the point of minimum potential energy.

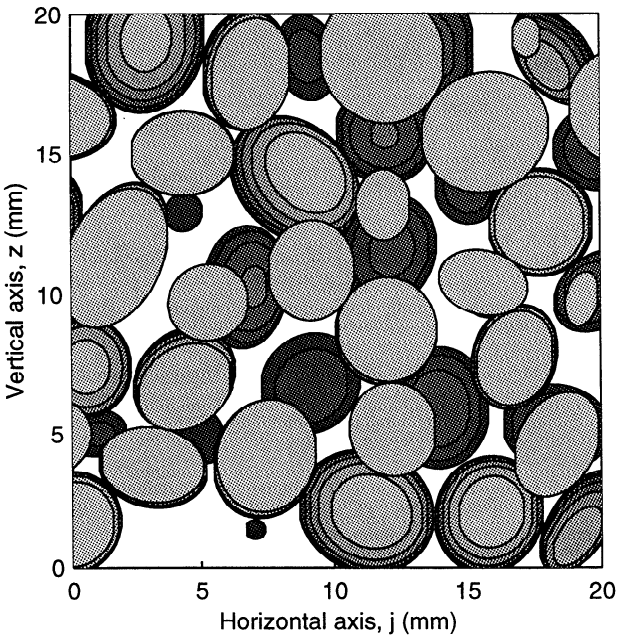

Figure 5. Demonstration of the three-dimensional packing algorithm. Shown are several slices taken out of a 50-mm^3 cube filled with ellipsoidal particles with radii of 2mm ± 0.4 mm. Shading varies from light to dark to indicate increasing depth in the cube for a range of 2mm. This simulation using 3300 particles took approximately 12 min using four processors of an IBM SP Parallel computer. Particles of arbitrary shape may be modeled at minimal additional computation cost.

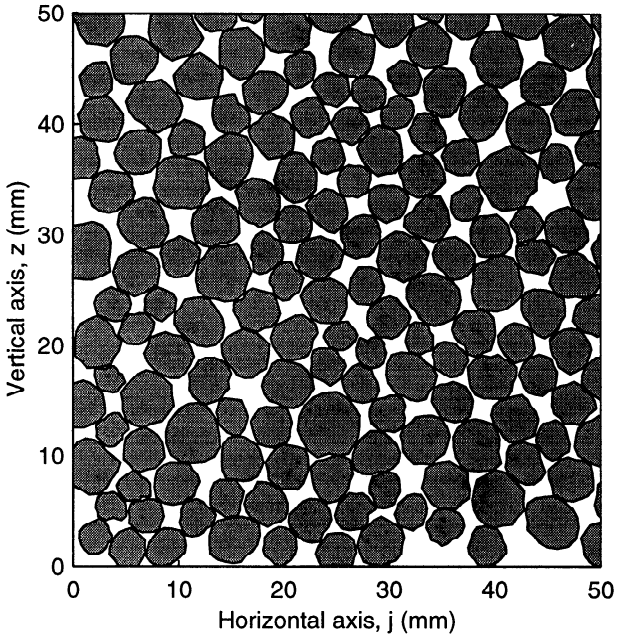

Figure 6. Demonstration of the packing algorithm for two-dimensional rocks. Rock surfaces are generated by a random walk about a uniform radius 2mm ± 0.4mm. This particular simulation of 100 × 100 mm took approximately 30 s on a Sun 10 workstation.

imization. Other natural substances, such as snow, may also be simulated by reducing the minimization of potential energy constraint, which can be accomplished by making individual particles stick once they reach the surface of the packed layer. The simplicity with which the algorithm can be changed for particles with a general cross section is demonstrated in Figure 6 where packing of two-dimensional rocks is simulated. In this figure the standard packing algorithm is used with a random walk modification of the individual particle surfaces.

3. Permittivity Correlation and Pair Distribution Functions

One of the principal uses of the packing algorithm is in the calculation of the permittivity correlation and pair distribution functions which can be used in conjunction with coherent theoretical approaches to compute scattering in inhomogeneous random media. One such classical approach is the Born approximation (Figure 7) [*Tsang et al.*, 1985], where the permittivity fluctuations act as distributed sources in an effective homogeneous medium. The scattering

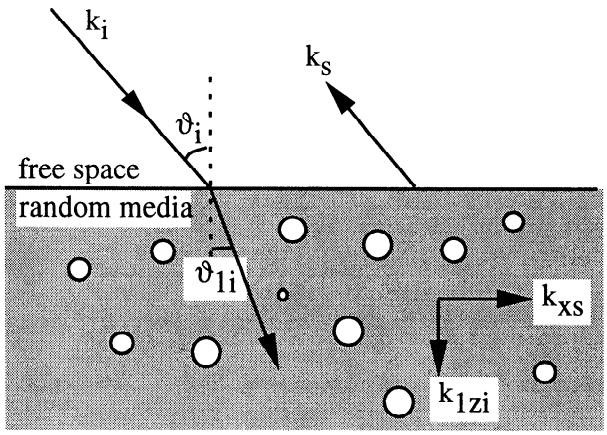

Figure 7. Geometry for a two-dimensional random medium. Medium 0 is considered free space, and medium 1 is a random media consisting of particles as described in Figure 4.

solution is then determined using a perturbation series. It is shown that for a random medium where the variation of the fluctuating permittivity is relatively small, the scattering coefficient from the medium can be directly calculated from the Fourier transform of the correlation function given by

$$C(\overline{r}-\overline{r}') = \langle \epsilon_f(\overline{r})\epsilon_f(\overline{r}')\rangle \tag{6}$$

where $\epsilon_f(\overline{r})$ is the fluctuating part of the permittivity function. The most commonly accepted form for the correlation function is the exponential function which was derived originally by *Debye et al.*[1957] for a sparse random collection of spherical particles and is given by

$$C(\overline{r}) = e^{-|\overline{r}|/r_0}. \tag{7}$$

The corresponding two-dimensional power spectral density is given by

$$\phi(\overline{k}) = \frac{r_0^2}{(1+r_0^2|\overline{k}|^2)^{3/2}}. \tag{8}$$

Here, the parameter $\overline{r}_0$ is related to the mean diameter of particles in the random medium. For dense random media, experimental and numerical methods have been attempted to determine $C(\overline{r}-\overline{r}')$ from the recorded samples of the medium under study. For most practical cases, the behavior of the correlation function when $\overline{r}'$ is in the near vicinity of $\overline{r}$ does indeed resemble that of an exponential or Gaussian function. Because of the ease with which these functions can be manipulated algebraically, their use has become widely prevalent in the literature. A difficulty that arises however, is that the power spectral density is proportional to the integral of the correlation function over all space, and thus estimation of the correlation function for only small values of $\overline{r}-\overline{r}'$ may not be sufficient for accurate estimation of the power spectral density for different ranges of observing frequencies.

The packing algorithm described in the previous section is an ideal tool for determining the validity and range of applicability of assumptions made in the determination of this correlation function. Furthermore, since the packing algorithm is capable of making a full Monte Carlo realization of a random medium, it may be used to enhance the understanding of the physics behind the scattering mechanisms in a very dense medium. Computationally, it is much faster to perform simulations in two dimensions to first develop an understanding and then in the future to extend the results to three dimensions. In two dimensions, it can be shown that the radar cross section using the Born approximation is given by

$$\begin{aligned}
\sigma^o_{vv}(\theta_i) &= |X_{01i}|^4\mathcal{K} \\
\sigma^o_{hh}(\theta_i) &= \frac{k_0^4}{k_1^4}|Y_{01i}|^4\mathcal{K} \\
\mathcal{K} &= \frac{2\pi^2 k_0^3\phi(2k_{xi},-2k_{1zi})}{\cos(\theta_i)(2k''_{1zi})}\left|\frac{k_{zi}}{k_{1zi}}\right|^2 \\
k_{xi} &= k_0\sin(\theta_i) \\
k_{1zi} &= k_{1m}\cos(\theta_i)
\end{aligned} \tag{9}$$

where θ_i is the angle of incidence, X_{01i} and $\frac{k_0}{k_1}Y_{01i}$ are the transmission coefficients from medium 1 to medium 0, k_{1m} is the mean field propagation constant due to the average dielectric, $\langle\epsilon\rangle$, k''_{1zi} is the imaginary part of the propagation constant in the scattering medium and the power spectral density ϕ is

$$\phi(k_x,k_z) = \frac{1}{(2\pi)^2}\int C(\overline{r}-\overline{r}')e^{i\overline{k}\cdot\overline{r}}d^2r. \tag{10}$$

The unknowns in this formulation are the propagation constant and the correlation function for the random medium. The propagation constant can be either the spatial average of the dielectric constant within the random medium (Born approximation) or derived from a mixing formula (distorted Born approximation). In what follows, the Born approximation will be developed for a prototypical example in which the described packing algorithm will be used to provide the correlation function. After illustrating the two-dimensional correlation function with the associated power spectral density, a comparison will be made with similar results obtained by using an exponential correlation function (7) having the same correlation length. In the calculation of the permittivity fluctuation correlation function from the collected samples of the medium, it is common to generate the autocorrelation function of each sample and then average the resultant autocorrelation functions. However, a difficulty may arise from this procedure: the Fourier transform of the correlation function may become negative over some partial frequency range. This is a result of poor estimation of the tail of the correlation function and possible asymmetry in the sample cross section, the former being a consequence of the finite size of the sampled medium. To circumvent this difficulty while keeping the size of the sampled medium within realis-

tic dimensions, the power spectral density should be computed directly from the Fourier transform of a profiled sample of the random medium. Since the correlation function of the permittivity fluctuation process is continuous, it implies that the process is continuous in the root mean squared sense, which in turn implies that the power spectral density can be directly computed from

$$\phi(k_x, k_z) = \lim_{\substack{X \to \infty \\ Z \to \infty}} \left\{ \frac{1}{XZ} E \left| \int_0^X \int_0^Z \epsilon_f(x,z) e^{i(k_x x + k_z z)} dx dz \right|^2 \right\}. \quad (11)$$

The example considered here simulates the observation of a two-dimensional layer of sand particles with permittivity $\epsilon_s = 3.15 + j0.005$, $\langle \epsilon \rangle = 2.54 + j0.004$, $\langle \epsilon_f^2 \rangle = 0.56$, and volume fraction $f = 0.8$. Individual realizations of Gaussian-distributed packed particles were created using a mean radius r =2 mm with a standard deviation of 0.4 mm for the two principal axes and a uniform distribution for the orientation angle of the ellipses. Observation frequencies used for this discussion will be at a below-resonance frequency of 10 GHz ($\lambda_s/2 = 8.5$mm) and an above-resonance frequency of 35 GHz ($\lambda_s/2$ = 2.4mm), where resonance refers to the average half wavelength ($\lambda_s/2$) dimension of the scattering particles. Over three hundred packing realizations of the dimensions 0.2 x 0.2 m were used to determine the power spectral density directly from the Fourier transform of the packed profiles given by the packing algorithm. The correlation function and the power spectral density are shown in Figures 8 and 9, respectively, where the nonaxial symmetry patterns are clearly displayed. The strongest peak in the power spectral density lies along the diagonal, as would be expected in a tightly packed array of two-dimensional spheres with a narrow size distribution. A wider distribution would give a more axially symmetrical two-dimensional spectrum.

This can be demonstrated by using a Rayleigh distribution to determine particle radius rather than using a Gaussian distribution. Because the packing algorithm has a limited resolution due to the discretization of the particle ((2) and (3)), the Rayleigh distribution is truncated at the very small scale. Furthermore, for the sake of comparison with previous theoretical and experimental work, particle shapes used with the Rayleigh distribution were made circular rather than elliptical, this has the effect of reducing the randomness of particle locations, but this is an effect that is ameliorated by the wider particle size distribution.

The probability density functions of both distributions are shown in Figure 10, where it can be seen that the Rayleigh distribution is wider by about a factor of three. Thus for the wider particle size distribution we would expect that the correlation function and spectral density to more closely approximate

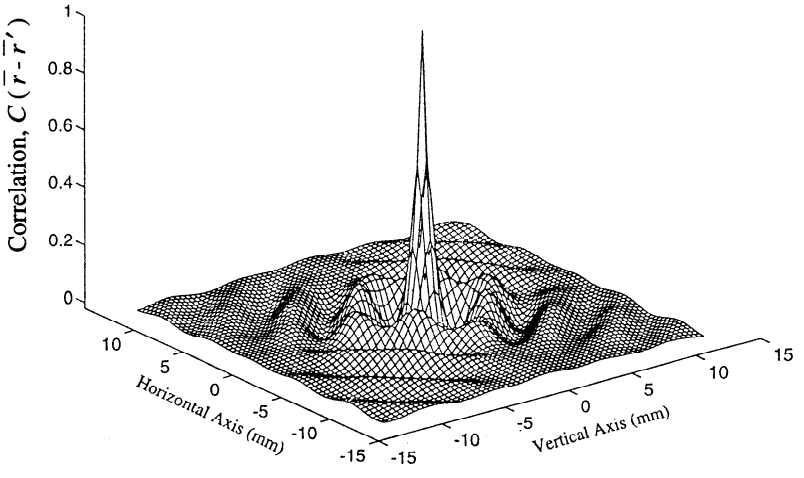

Figure 8. Two-dimensional correlation function for the particles in Figure 4. The correlation function is not axially symmetrical.

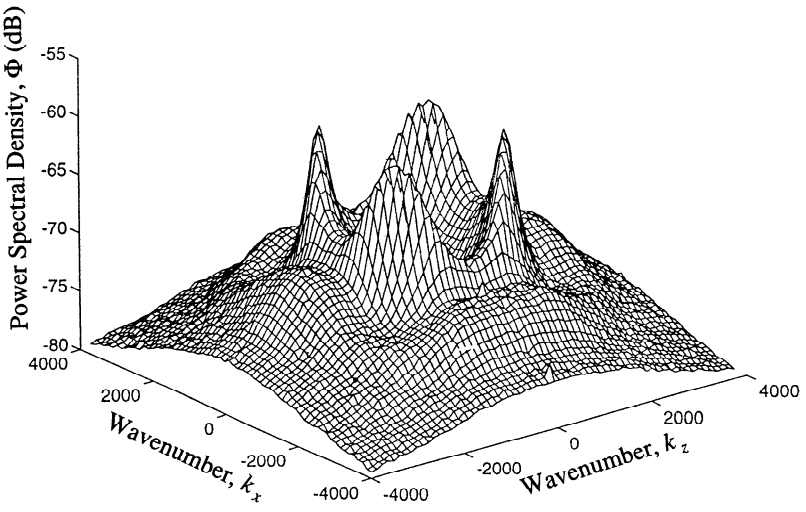

Figure 9. The power spectral density derived from data shown in Figure 4. Strong peaks along the diagonal highlight the periodicity in the correlation function seen along this axis. Arcs drawn along a constant radius are proportional to the backscatter intensity as a function of incidence angle.

that of the exponential function (which would be correct for completely random particle placement) and this is indeed shown to be the case. Plots in Figures 11a through 11c illustrate the correlation function and its power spectral density along three principal axes of the two-dimensional volume for both particle distributions and the exponential correlation function. It can be seen that at both short and long distances, the correlation function of both particle distributions and the theoretical exponential function agree very well, but it is at the midrange distances where the functions can be seen to differ. These differences become more apparent in the low-frequency region of the power spectral density for the derived correlation functions. Note again a better agreement of the Rayleigh-distributed particle result with the theoretical exponential function, but still there is an appreciable error at the low-frequency region.

Referring to the Gaussian distribution function, the effect of the strong peaks in the power spectral density function along the XZ axis in Figure 11b can be clearly seen in the extended periodicity of the correlation function along this axis. Again, this is indicative of the natural ordering of the system for tightly packed arrays of particles with a narrow particle size distribution, and we note that it is less of a feature when the particle sizes follow a Rayleigh distribution. An important consequence of this lack of symmetry, however, is that it would be inappropriate to calculate the correlation function along one axis of the distribution (such as the function in Figure 10a) and to enforce axial symmetry. The effect of such an action would be that the resulting power calculated through (10) would not be positive for all frequencies because the chosen correlation function along the one axis is not, and cannot be, the correlation function for an axially symmetrical medium. In effect, then, if an exponential or Gaussian function is not to be used, the only appropriate way to calculate the correlation function is to completely sample the fluctuations in two- or three-dimensional space.

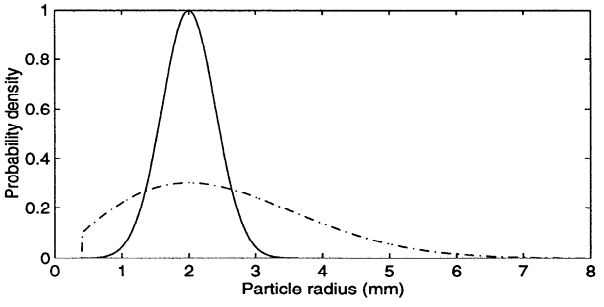

Figure 10. Gaussian (solid line) and truncated Rayleigh (dot-dashed line) probability distribution functions of particle radii used in the packing algorithm. Both distributions have the same mean.

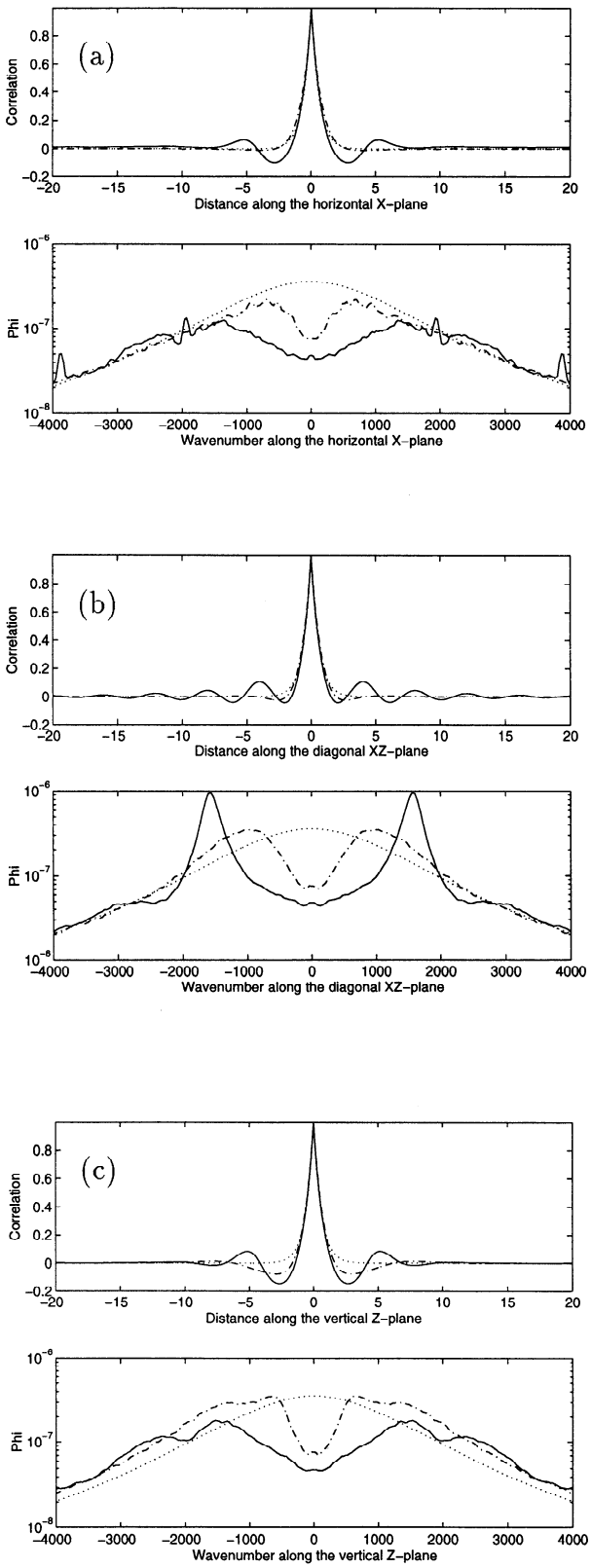

Furthermore, and more importantly, as is shown by Figures 11a through 11c, the deviation of the numerically derived power spectral density from the exponential power spectral density is as high as an order of magnitude at the lower frequencies, which is precisely the region of validity for the Born approximation.

As indicated by (9), only a portion of $\phi(k_x, k_z)$ is "visible" at a particular frequency. The loci of the spatial frequencies as the incidence angle varies from 0^o to 90^o is an ellipse with semi-axes of $2k_0$ and $2k_{1m}$, as illustrated in Figure 12. In this figure it can be seen that while the spectral density is not axially symmetric, the visible regions at each of the observing frequencies are nearly so. The effects of the asymmetry are most strongly observed at frequencies near the resonance of the particles within the medium. This figure can be used to understand the relationship between observing frequency and physical structure of a random medium. Decreasing particle sizes would have the effect of moving features radially outward in the figure, the same effect as decreasing frequency. Narrowing the particle distribution would have the effect of increasing the magnitude of the peaks shown in the figure and further disturb the high-frequency agreement of the observed backscatter with the backscatter response expected for a medium whose particles follow an exponential function. Another interpretation of the figure shows that the particle size distribution of a random medium may be explored by frequency sweeping near the particle resonance at angles slightly greater than 45°.

Given the derived correlation function for a specific particle size distribution we can carry out the remaining mathematical operations in (9) to get the observed backscattering cross section, which is shown in Figures 13 and 14. In Figure 13 the backscattering coefficients of the medium for both the vertical and horizontal polarizations at 10 GHz and 35 GHz are shown and compared with those derived based on an exponential correlation function for a Gaus-

Figure 11. Slices of Figures 8 and 9 taken along the principal axes of (a) $\theta = 0^o$, (b) $\theta = 45^o$, and (c) $\theta = 90^o$. The solid lines and the dot-dashed lines show the numerically derived values for the Gaussian and Rayleigh particle size distributions, respectively. The dotted lines show the equivalent correlation function and spectrum for the best fit exponential.

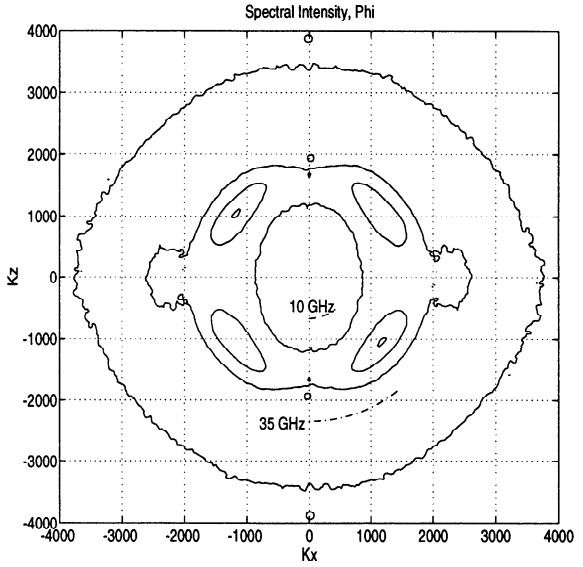

Figure 12. Illustration of the visible region of the Born approximation at two different frequencies shown overlaid on a contour map of the power spectral density (Figure 9) for the Gaussian particle size distribution. Note that the greatest angular variation due to the packing structure occurs near resonance at $f = 21$ GHz.

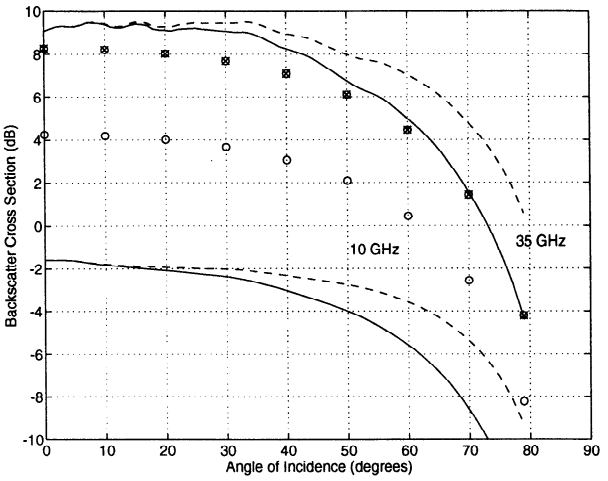

Figure 13. Results of the two-dimensional Born approximation for both 10 and 35 GHz for the Gaussian particle size distribution. Solid lines are for vertical polarization, dashed lines are for horizontal polarization, and the open and crossed-out circles indicate vertically polarized results of the Born approximation using the best-fit exponential (Figure 11).

sian particle size distribution. Figure 14 is the same as Figure 13 for an observation frequency at particle resonance (21 GHz), where differences between observed and predicted backscatter response are expected to be the greatest.

Referring to Figures 8 through 14, the following observations are in order: (1) differences between the backscattering coefficients estimated from the correlation function derived from the Monte Carlo simulation and the exponential function can be as high as 10 dB; (2) angular variation may depend strongly on the observation frequency and particle size distribution (see Figure 14); and (3) the correlation function and the respective power spectral density are not likely to be radially symmetrical, but this may not have a strong effect on the observation with the exception of frequencies near resonance.

Another statistical function relating to particle positions that is commonly used in the study of random media is that of the pair distribution function, $p(\overline{r}_j|\overline{r}_i)$, which is the probability of finding a particle located at a position $\overline{r}_j$, given a particle located at position $\overline{r}_i$ [*McQuarrie*, 1976]. The knowledge of the pair distribution function becomes necessary where the effective propagation constant of a dense random media is to be determined [*Tsang et al.*, 1985; *Lax*, 1952]. As the packing algorithm can be used to determine the correlation function, it can also be used to determine the pair distribution function.

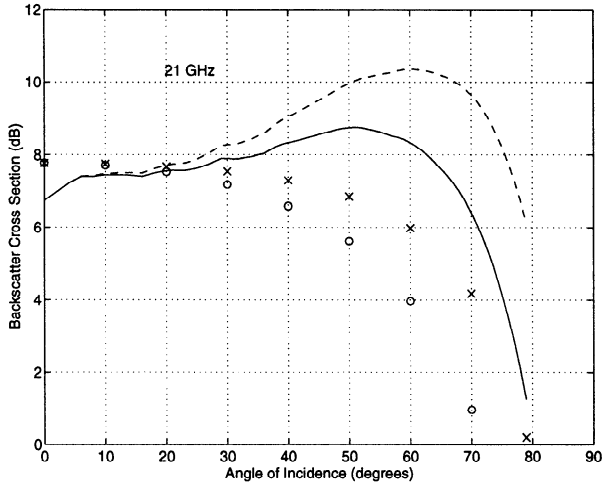

Figure 14. Results of the two-dimensional Born approximation at particle resonance ($f = 21$ GHz) for both numerically derived (Gaussian particle size distribution) and exponential correlation functions. Solid lines and circles indicate vertical polarization, and dashed lines and crosses indicate horizontal polarization. The symbols represent the theoretical exponential curves in both cases.

Figure 15 illustrates the aggregate pair distribution function for the particle arrangement consisting of two-dimensional ellipses shown in Figure 4. In this figure, the pair distribution function is shown as a gray scale image in two dimensions where the brightness is directly proportional to the probability. As expected, a dark area covers the central region indicating the zero probability of having two particles intersecting one another. More remarkable is the ringing effect along the diagonals of the image, indicating periods of high and low probability, which is reflective of the results obtained by the correlation function. This effect is highlighted in the graph inset in Figure 15, where the pair distribution function is shown quantitatively along the horizontal, vertical, and diagonal axes. The strong peaks along the diagonal axis are a result of the dense packing with a narrow size distribution. In comparison, the Percus-Yevick pair distribution function predicts an axially symmetrical function for single-sized spherical particles. The example given here clearly is not so and cannot be so for monosized particles under the influence of gravity. This does not disprove the Percus-Yevick pair distribution function, but it does call into question its application to macroscopic granular media under the influence of external forces.

Additional treatment of the sensitivity of the pair distribution function to particle extraction is given in the Appendix. In this treatment it is shown how the pair distribution function does not change when particles are randomly removed from a simulated arrangement of particles. The central assumption to this observation is that when particles are removed, the remaining particles are not allowed to phyically rearrange themselves. This is an arguably unphysical phenomenon, but it emphasizes how similar arrangements of particles may result in considerably different pair distribution functions. This point is especially

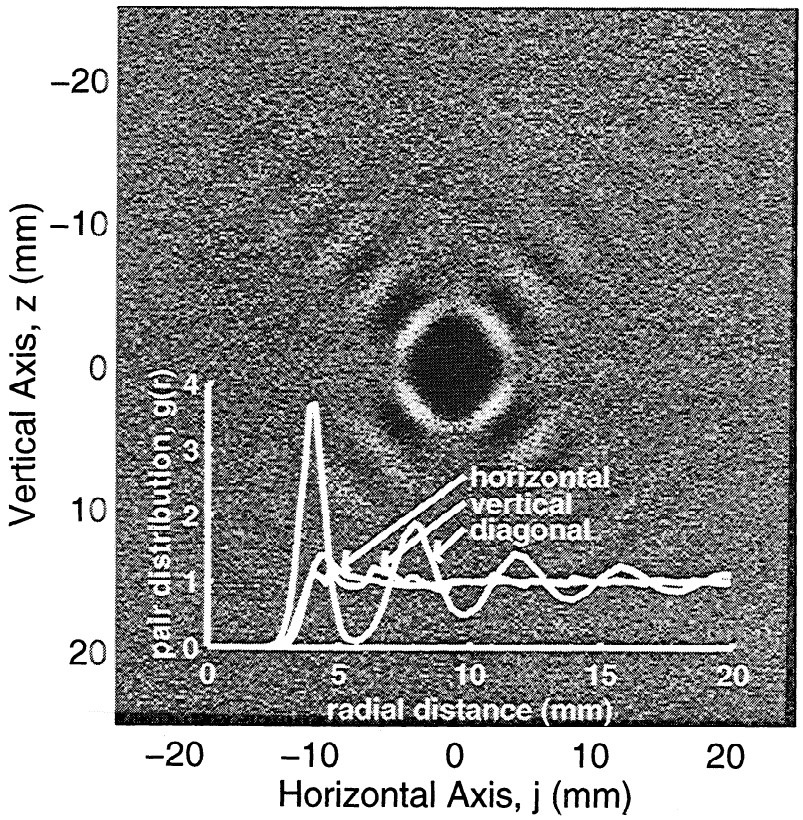

Figure 15. The pair distribution function, $p(\overline{r}_j|\overline{r}_i)$, for the packed array shown in Figure 4 (Gaussian size distribution). Dark areas indicate low probability and bright areas indicate a high probability of finding another particle at $\overline{r}_j$, given a particle at $\overline{r}_i$. The inset graph gives the quantitative pair distribution function along the vertical, horizontal, and 45° axes.

important for those who use the Percus-Yevick pair distribution function in the modeling of snow.

4. Conclusions

In this paper we have introduced a new approach to determining particle arrangements. The approach is computationally efficient, flexible, and was demonstrated to work in two dimensions as well as three for nonspherical particles. A two-dimensional "rocks" example was also given that demonstrated the ability of the algorithm to work with particles of arbitrary shape. The algorithm was then used to compute the correlation function for two different size distributions of particles, one Gaussian and the other Rayleigh, and it was highlighted that the proper way to calculate the correlation function was through an averaged periodogram in the spectral domain rather than averaging individual correlation functions or assuming radial symmetry from the outset. The correlation functions of the two particle size distributions were compared with a theoretical exponential correlation function, where it was shown that the derived functions deviated from the theoretical at low frequencies but agreed well at high frequencies. It was also shown that the wider Rayleigh distribution gave a better fit overall to an exponential function, as would be expected.

Derived correlation functions from the packing algorithm were used to compute radar backscatter via the Born approximation, where it was shown that an increase in the backscatter response as a function of observation angle can be related to angular asymmetry in the correlation function. This asymmetry may be due to the natural ordering of particles when arranged under the influence of gravity. Finally, another application of the packing algorithm was given as it applies to the determination of the particle pair distribution function, which is a key unknown in the quasi-crystalline approximation, and an argument was presented as to why the more common Percus-Yevick pair distribution function is not appropriate for use with granular media.

Appendix

As mentioned in the main body of the paper, the pair distribution function plays an important role in many field theories of scattering behavior. Often this is thought of as being a robust quantity and the pair distribution function of one medium is applied to another with the hopes that the pair distribution function would still be applicable. For instance, it is very common to apply the Percus-Yevick pair distribution function for classical fluids to the problem of snow [*Wen et al.*, 1990; *Tsang and Kong*, 1992; *Tsang*, 1992]. In fact, the pair distribution is very dependent on the method of particle arrangement as was illustrated in Figure 15. One interesting aspect of the pair distribution is that it remains unchanged under the process of particle extraction (assuming that particles are not allowed to rearrange themselves). The example given here highlights how similar arrangements of particles may result in strikingly different pair distribution functions.

In general, the pair distribution function may be written as [*McQuarrie*, 1976, pg. 258]

$$g(\overline{r}_2, \overline{r}_1) = p(\overline{r}_2|\overline{r}_1)/p(\overline{r}_1), \tag{12}$$

where $p(\overline{r}_2|\overline{r}_1)$ is the probability of a particle being located at $\overline{r}_2$ given a particle located at $\overline{r}_1$, and $p(\overline{r}_1)$ is equal to the particle number density, n_0. Note that when $|\overline{r}_2 - \overline{r}_1| \gg b$ (where b is the average grain diameter), $p(\overline{r}_2|\overline{r}_1) = p(\overline{r}_1)$, and then $g(\overline{r}_2, \overline{r}_1) = 1$, as expected. Now, given a particular particle arrangement method (say, a classical fluid), we have the probability function

$$p_0(\overline{r}_2|\overline{r}_1). \tag{13}$$

If we reduce the particle density in our system by the factor f, we have

$$p_0'(\overline{r}_1) = f p_0(\overline{r}_1) \tag{14}$$

and similarly (because particle removal is independent of particle position),

$$p_0'(\overline{r}_2|\overline{r}_1) = f p_0(\overline{r}_2|\overline{r}_1). \tag{15}$$

Then by (12), the pair distribution function remains unchanged.

This result can be easily demonstrated numerically by generating random arrangements of particles. A common method of simulating a classical fluid is to randomly introduce particles into an empty container (Figure A1). In Figure A1a, the particles represented by dotted lines illustrate a classical fluid simulation for a volume fraction of 30%. The particles represented by solid lines in Figure A1a show the remaining particles after reducing the number of particles

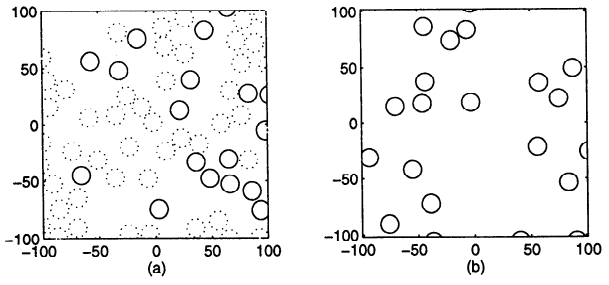

Figure A1. Particle arrangement method for a classical fluid. (a) 30% volume fraction using sequential addition (dotted circles) and 10% volume fraction resulting from particle extraction (solid circles). (b) 10% volume fraction using sequential addition.

from a volume fraction of 30% to a volume fraction of 10% by random extraction. Figure A1b gives a classical fluid distribution of particles for a volume fraction of 10% where, as for the 30% case, particles have been randomly placed in the box but not removed. The pair distribution function for these different methods is given in Figure A2.

Clearly, the pair distribution of the 10% volume fraction obtained from extraction yields the same pair distribution function obtained from the 30% classical fluid simulation. These pair distribution functions are distinctly different from the function obtained for the 10% classical fluid simulation. The reason that the two simulations for 10% volume fraction differ is that in the particle extraction case, particles are randomly removed, regardless of their position. When creating the 30% volume fraction simulation (from which the extraction example was derived), particles are occasionally excluded if they overlap, and it is this exclusion process which makes

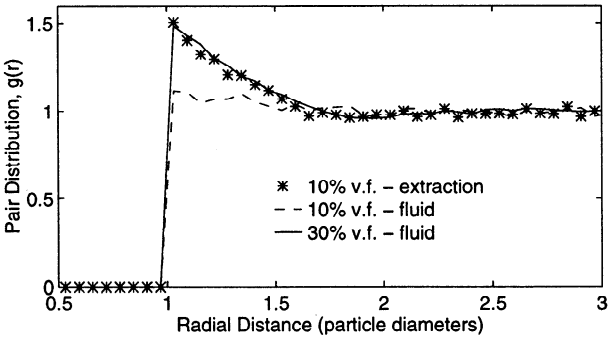

Figure A2. Comparison of the different pair distribution functions obtained from simulations demonstrated in Figure A1.

the classical fluid pair distribution functions different for the 30% and the 10% volume fractions. Reducing the number of particles does not alter the effect of this exclusion process. Thus, the fact that the pair distribution function does not change when particles are extracted has been shown both theoretically and by example.

Acknowledgments. Computing services were provided by the University of Michigan Center for Parallel Computing, which is partially funded by NSF grant CDA-92-14296. The authors also wish to thank the reviewers for the valuable comments and suggestions.

References

Appleton, P. N., P. R. Siqueira, and J. P. Basart, A morphological filter for removing "cirrus-like" emission from far-infrared extragalactic IRAS fields, *The Astron. J., 106*(4), 1664–1678, 1993.

Broyles, A. A., S. U. Chung, and H. L. Sahlin, Comparison of radial distribution functions from integral equations and Monte Carlo, *J. Chem. Phys., 37*(10), 2462–2469, 1962.

Buchalter, B. J., and R. M. Bradley, Orientational order in random packings of ellipses, *Phys. Rev. Ser. A, 46*(6), 3046–3056, 1992.

Buchalter, B. J., and R. M. Bradley, Orientational order in amorphous packings of ellipsoids, *Europhys. Lett., 26*(3), 159–164, 1994.

Chandrasekhar, S., *Radiative Transfer*, Dover, Mineola, N. Y., 1960.

Debye, P., H. R. Anderson, and H. Brumberger, Scattering by an inhomogeneous solid, II, The correlation function and its applications, *J. Appl. Phys., 28*(6), 679–683, 1957.

Ding, K. H., C. E. Mandt, L. Tsang, and J. A. Kong, Monte Carlo simulations of pair distribution functions of dense discrete random media with multiple sizes of particles, *J. of Electromagn. Waves Appl., 6*(8), 1015–1030, 1992.

Giardina, C. R., and E. R. Dougherty, *Morphological Methods in Signal and Image Processing,* Prentice Hall, Englewood Cliffs, N. J., 1988.

Lax, M., Multiple scattering of waves, II, The effective field in dense systems, *Phys. Rev., 85*(4), 621–629, 1952.

McQuarrie, D. A., *Statistical Mechanics,* HarperCollins, New York, 1976.

Percus, J., and G. Yevick, Analysis of classical statistical mechanics by means of collective coordinates, *Phys. Rev., 110*, 1–13, 1958.

Serra, J. P. *Image Analysis and Mathematical Morphology,* Academic, New York, 1982.

Tsang, L., Dense media radiative transfer theory for

dense discrete random media with particles of multiple sizes and permittivities, in *Progress in Electromagnetics Research*, Elsevier, New York, 1992.

Tsang, L., and A. Ishimaru, Radiative wave equations for vector electromagnetic propagation in dense nontenuous media, *J. Electromagn. Waves Appl., 1*(1), 59–72, 1987.

Tsang, L., and J. A. Kong, Scattering of electromagnetic waves from a dense medium consisting of correlated Mie scatterers with size distributions and applications to dry snow, *J. Electromagn. Waves Appl., 6*(3), 265–286, 1992.

Tsang, L., J. A. Kong, and R. Shin, *Theory of Microwave Remote Sensing,* John Wiley, New York, 1985.

Vallese, F., and J. A. Kong, Correlation function studies for snow and ice, *J. Appl. Phys., 52*(8), 4921–4925, 1981.

Visscher, W. M. and M. Bolsterli, Random packing of equal and unequal spheres in two and three dimensions, *Nature, 239*, 504–507, 1972.

Wen, B., L. Tsang, D. Winebrenner, and A. Ishimaru, Dense media radiative transfer theory: comparison with experiment and application to microwave remote sensing polarimetry, *IEEE Trans. Geosci. Remote Sens., 28*(1), 46–59, 1990.

P. R. Siqueira, K. Sarabandi, and F. T. Ulaby, Radiation Laboratory, Department of Electrical Engineering and Computer Science, 3228 EECS Building, University of Michigan, Ann Arbor, Michigan 48109-2122. (e-mail: siqueira@eecs.umich.edu; sarabandi@eecs.umich.edu; ulaby@eecs.umich.edu)

(Received June 10, 1994; revised June 5, 1995; accepted June 12, 1995.)